J Wood Sci (2011) 57:247–253
DOI 10.1007/s10086-010-1165-7

NOTE

Yoshikazu Araki · Toshiki Endo · Manami Iwata

Feasibility of improved slotted bolted connection for timber moment frames

Received: August 23, 2010 / Accepted: November 9, 2010 / Published online: March 17, 2011

Abstract This note examines the feasibility of an improved slotted bolted connection for timber moment frames. In the improved connection, steel tubes are inserted into drill holes in glulam and fixed to the glulam with resin injection. Aluminum splice plates with curved slots, or curved elongated holes, are fastened mechanically by using high-strength bolts that go through the steel tubes. Since the compression due to bolt tension is fully supported by the steel tubes, the reduction of bolt tension due to shrinkage of the glulam can be avoided. The use of slotted aluminum splice plates allows stable energy dissipation due to smooth sliding between the aluminum splice plates and the end surfaces of the steel tubes within the specified range of rotation angle. Through quasistatic cyclic loading tests of two connection specimens, it was demonstrated that stable and nearly rigid–plastic hysteresis loops were obtained whose equivalent viscous damping ratio was more than 30% in the range of rotation angle close to or greater than 1/50 radian. Although further improvement is necessary, the experimental results demonstrate the feasibility and potential of the present connection.

Key words Timber moment frame · Slotted bolted connection · Friction damper · Steel tube · Resin injection

Introduction

The performance of timber connections under cyclic loading is one of the key factors that determine the overall seismic performance of a timber frame. A number of research works have been undertaken to improve the cyclic performance of timber connections.[1–7] Hysteresis loops of conventional bolted timber connections are often characterized by pinching, or degradation of stiffness and strength under cyclic loading. The main sources of pinching are enlargement of bolt holes, inelastic bolt elongation, or both. Pinching is undesirable because it leads to a reduction in energy dissipation capacity. Furthermore, pinching reduces the lateral stiffness of a timber frame, which may require significant repair after a strong earthquake.

As an approach to avoid pinching, the concept of the slotted bolted connection (SBC), originally developed as a friction damper for steel frames, was applied to timber connections.[5,6] In SBCs, steel plates with and without slots, or elongated holes, are fastened by high-strength bolts, and energy is dissipated by sliding between the steel plates. The application of SBCs to timber connections dates back at least to the work by Duff et al.[5] in the late 1990s. The problem of pinching remained in their SBCs, however, because the steel plates were connected to glulam using conventional bolted connections. Leichti et al.[6] developed improved SBCs for timber frames and demonstrated that pinching can be prevented in the SBCs using quasistatic cyclic loading tests. Nevertheless, in their SBCs, steel plates were directly connected to glulam using the frictional resistance developed by bolt tension. Hence the reduction of bolt tension due to shrinkage of glulam may lead to significant reduction of energy dissipating capacity.[7] Although the use of Belleville (cone disk) compression washers was proposed to avoid or minimize the reduction of bolt tension, the long-term reliability of such an approach is uncertain.

Apart from the SBCs mentioned above, two types of friction connections for timber frames have been developed[8,9] that can avoid the reduction of bolt tension due to shrinkage of glulam. Tokuda et al.[8] inserted steel tubes into oversized drill holes in glulam and fixed them by injecting epoxy resin between the glulam and the steel tubes. Suzuki et al.[9] pressed steel tubes into holes with a diameter slightly smaller than that of the steel tubes. In both of these connections, splice plates were fastened mechanically by high-strength bolts that went through steel tubes. This way, the compression due to bolt tension can be fully supported by the steel tubes, which makes the reduction of bolt tension negligible even in long-term use. It was shown through

Y. Araki (✉) · T. Endo · M. Iwata
Department of Architecture and Architectural Engineering, Kyoto University, Katsura, Nishikyo, Kyoto 615-8540, Japan
Tel. +81-75-383-2924; Fax +81-75-383-2924
e-mail: araki@archi.kyoto-u.ac.jp

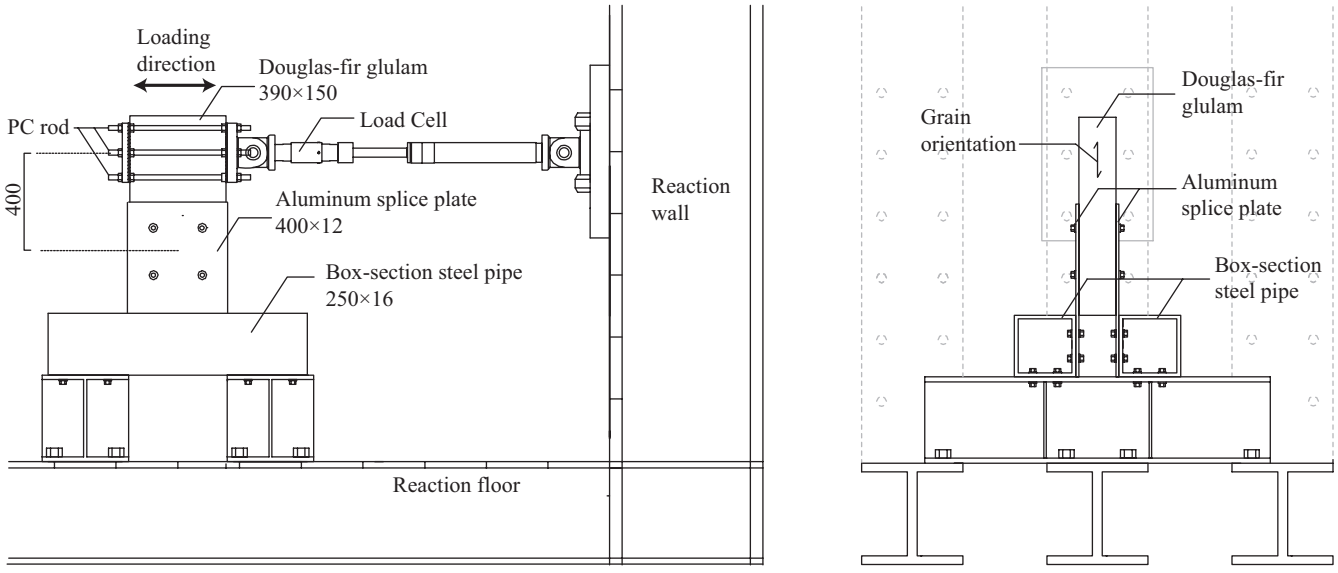

Fig. 1. Test setup of specimen A1. Dimensions are in millimeters

monotonic loading tests that the failure modes of both connections were ductile. Nonetheless, pinching is unavoidable in these connections since no slots were provided in the splice plates.

The objective of this note is to examine the feasibility of an improved SBC for timber moment frames that combines the strengths of, and eliminates the weaknesses of, the SBCs and the friction connections mentioned above. This note reports the results of quasistatic cyclic loading tests carried out to assess the performance of the present SBC.

Materials and methods

Figures 1 and 2 illustrate the experimental setup. Douglas-fir glulam was connected to box-section steel pipes using aluminum splice plates having curved slots. Cyclic loading was applied to the top of the glulam using a hydraulic actuator, while the box-section steel pipes were fixed to the reaction floor. Figure 3 shows schematically the initial and deformed configurations of a specimen. As shown in Fig. 4, steel tubes were inserted into holes drilled in the glulam, and epoxy resin was injected into the space between the steel tubes and the glulam. The aluminum splice plates were fastened mechanically to the glulam using high-strength bolts that went through the steel tubes. Two specimens, named specimens A1 and A2, were prepared for the tests. The differences between them were the numbers and locations of the steel tubes inserted in the glulam, as shown in Fig. 5.

Figure 6a shows a cut-open specimen after the test. The details of the build-up process were as follows.

1. A 40-mm-diameter hole was drilled and about half of the drill hole was widened so that the diameter of the wider side of the drill hole was 45 mm.
2. A steel washer was sandwiched by steel tubes P1 and P2, whose outer and inner diameters were 34 mm and 25 mm, respectively. They were bonded together using epoxy resin. The assembly of the steel washer and the steel tubes was inserted into the drill hole from the wider side.
3. Epoxy resin was injected into the space between P1 and the glulam. After the epoxy resin hardened, the specimen was reversed. Then epoxy resin was injected into the space between P2 and the glulam.

In addition to the above process, Steel tubes P1* and P2*, whose outer and inner diameters were 25 mm and 18 mm, were inserted as shown in Fig. 6b in this experiment to eliminate the difference between the inner diameter of the washer and those of P1 and P2. Note that these additional steel tubes, P1* and P2*, would have been unnecessary if the inner diameter of the washer had been equal to that of P1 and P2.

The cross section and length of the Douglas-fir glulam were 390 mm × 150 mm and 800 mm, respectively. The grade of the glulam was 10.5 GPa in terms of Young's modulus and 30.0 MPa in terms of flexural strength. The average moisture content and density of the glulam were 11.1% and 488 kg/m^3, respectively. The grade and the thickness of the aluminum splice plates were A2017P (JIS H4000)[10] and 12 mm. Curved slots, or curved elongated holes, of 18 mm width were predrilled in the splice plates as shown in Fig. 3 so that the allowable relative rotation angle was equal to 1/20 radian. No surface treatment was performed on the aluminum splice plate. Note that, although aluminum was selected as the material for the splice plates in this article to realize smooth sliding,[11] other materials could be used so long as smooth sliding is obtained. The grade of all the steel tubes was SS400 (JIS G3101).[12] The grade and diameter of the high-strength bolts were F10T

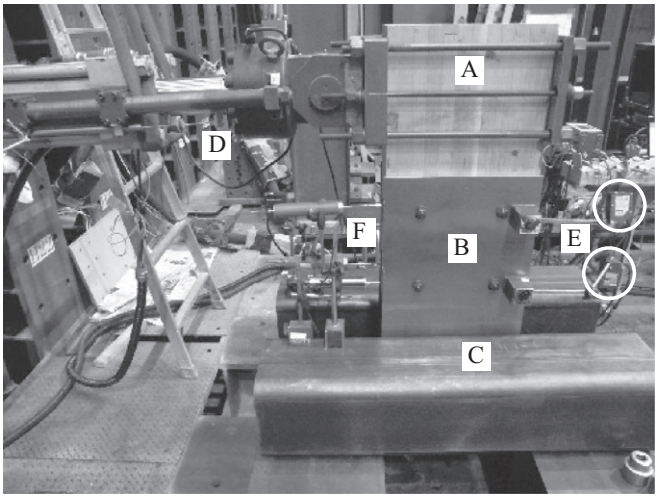

(a)

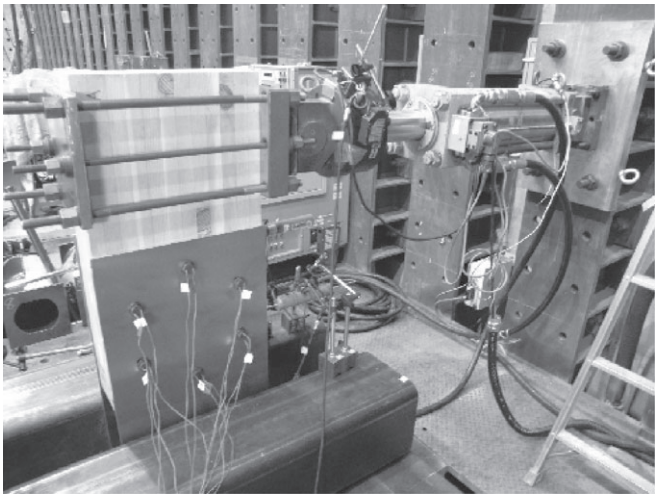

(b)

Fig. 2. Photograph of specimen A1 (**a**) and A2 (**b**) in the test rig. *A*, Douglas-fir glulam; *B*, aluminum splice plate; *C*, box-section steel pipe; *D*, load cell; *E*, laser displacement sensors (*circled*); *F*, displacement sensors

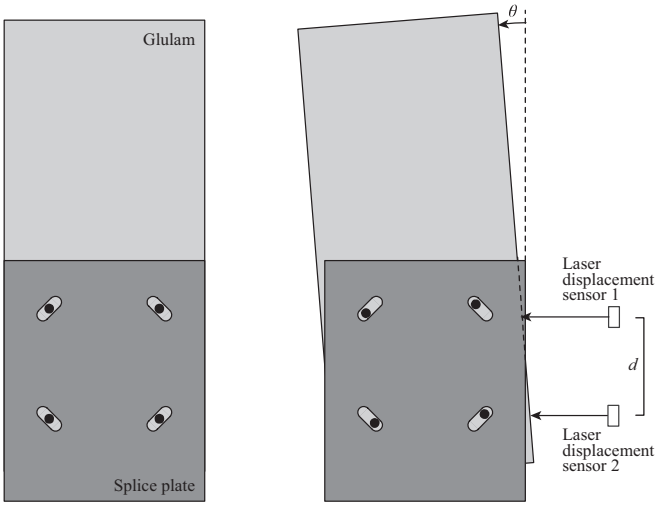

Fig. 3. Configurations of the specimen: **a** initial configuration, **b** deformed configuration. The curved slots predrilled in the splice plates are shown by *light gray elongated circles*, and the high-strength bolts going through the drill holes of the glulam are shown by *black circles*

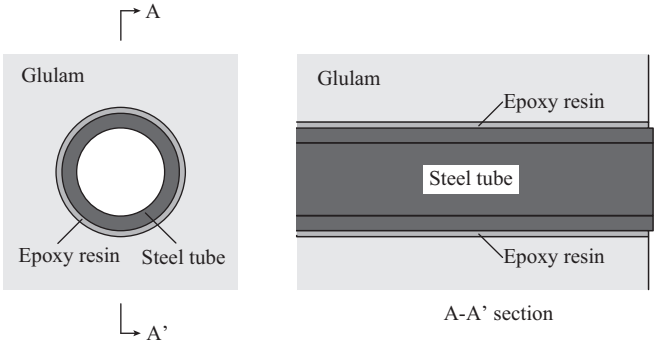

Fig. 4. Schematics of resin injection between steel tube and glulam

(JIS B1186)[13] and 16 mm. The grade of the epoxy resin was 9.1 MPa in terms of shear bond strength. The steel tubes were soaked in hydrochloric acid for 12 h as a surface treatment to increase the bond strength. The average friction coefficient between the end surfaces of the steel tube and the aluminum splice plate was found to be 0.30 in the material tests.

Cyclic horizontal forced displacement was applied at the top of the glulam using a hydraulic actuator as shown in Figs. 1 and 2. The amplitude ψ of the forced displacement was increased in the series 1.67, 3.33, 6.67, 13.33, and 20.00 mm, and three cycles of loading was repeated for each amplitude. The amplitude was determined so that ψ/h corresponds to 1/240, 1/120, 1/60, 1/30, and 1/20 radian, where h (= 400 mm) is the distance between the position of the actuator and the center of rotation, as illustrated in Fig. 1. The loading rate of the forced displacement was 0.1 mm/s.

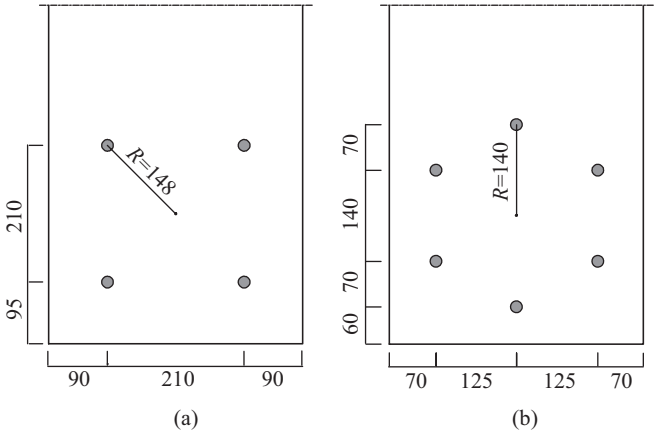

Fig. 5. Locations of the steel tubes: **a** specimen A1, **b** specimen A2. Dimensions are in millimeters

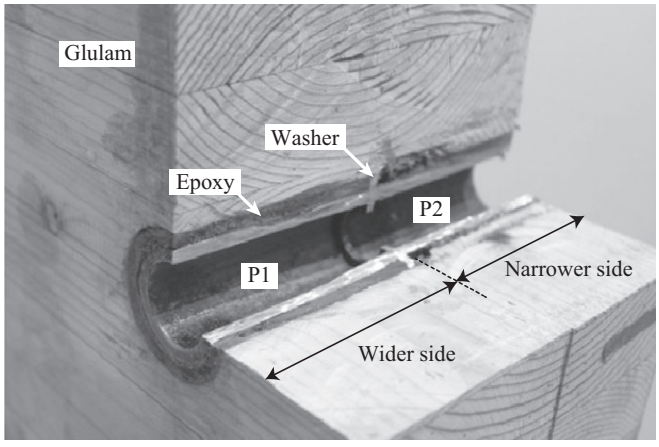

(a)

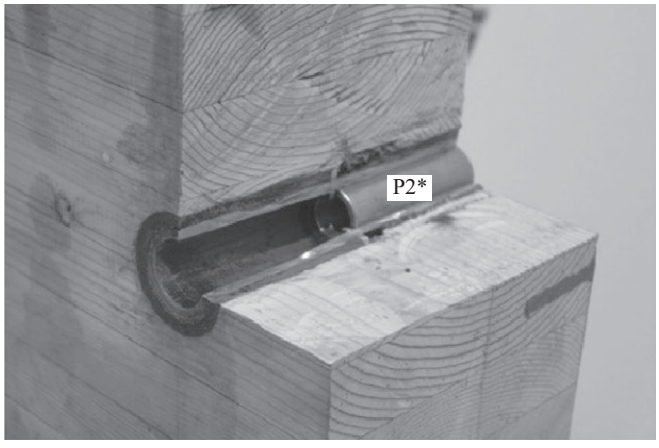

(b)

Fig. 6. Cut-open specimens after the tests: **a** basic composition, **b** insertion of additional pipe. *P1*, *P2*, identical steel tubes; *P2**, a steel tube inserted into P2 with the same inner diameter as the washer

The aluminum splice plates and the box-section steel pipes were fixed to the reaction floor as shown in Fig. 1.

Figure 3b schematically depicts the measurement of the relative rotation angle θ between the glulam and the aluminum splice plate. Laser displacement sensors were fixed to the aluminum splice plate as shown in Fig. 2. The relative rotation angle θ can be obtained as:

$$\theta = \frac{u_1 - u_2}{d} \tag{1}$$

where u_1 and u_2 indicate the displacement measured by laser displacement sensors 1 and 2, respectively, and d is the distance between the two laser displacement sensors. The values of d were 255 mm and 165 mm for specimens A1 and A2, respectively. In addition, displacement sensors were placed to measure the relative displacement between the aluminum splice plates and the box-section steel pipes, as shown in Fig. 2, to ensure no relative displacement took place between the aluminum splice plates and the box-section steel pipes. The applied moment M was obtained as:

$$M = Ph \tag{2}$$

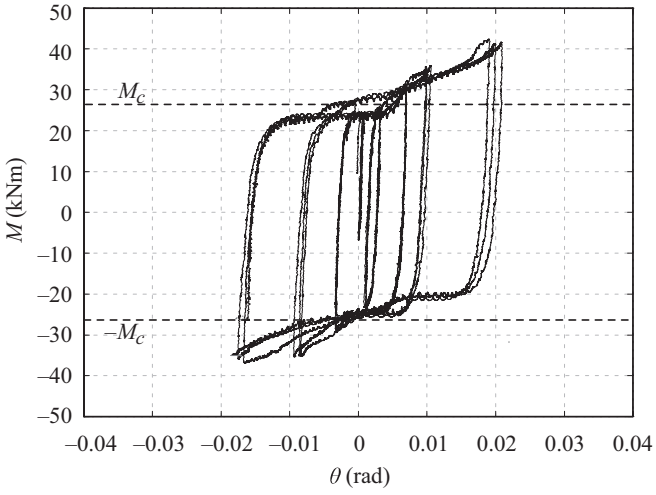

Fig. 7. Relationship between the moment (M) and relative rotation angle (θ) for specimen A1. M_c, estimate of the moment capacity

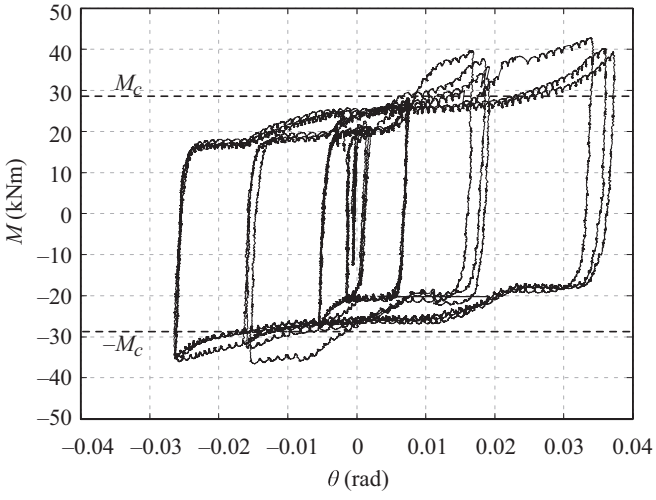

Fig. 8. Moment–relative rotation angle relationship for specimen A2

where P is the applied horizontal load measured by the load cell mounted on the actuator as shown in Figs. 1 and 2. As shown in Fig. 2b, the bolt tension was monitored by using strain gages attached inside holes drilled in the center of the high-strength bolts.[6]

Results and discussion

Figures 7 and 8 illustrate the relationship between the applied moment M and the relative rotation angle θ between the glulam and the splice plates. The estimates of the moment capacity M_c are also shown by dotted lines in Figs. 7 and 8. For specimens A1 and A2, M_c was 26.5 and 28.6 kNm, respectively. These values were obtained as:

$$M_c = n\mu TR, \tag{3}$$

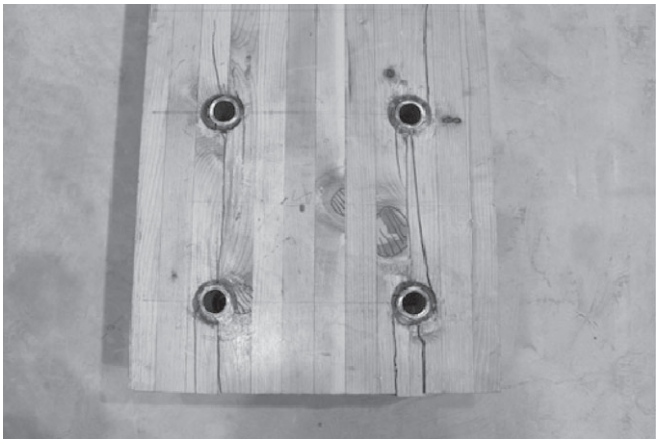

(a)

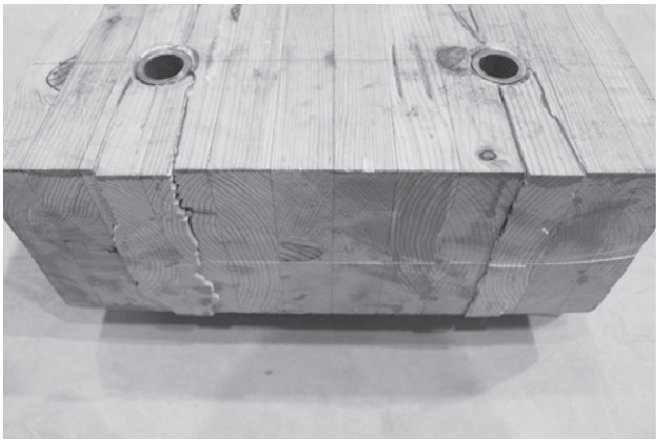

(b)

Fig. 9. Specimen A1 after the test: **a** side view, **b** side and bottom view

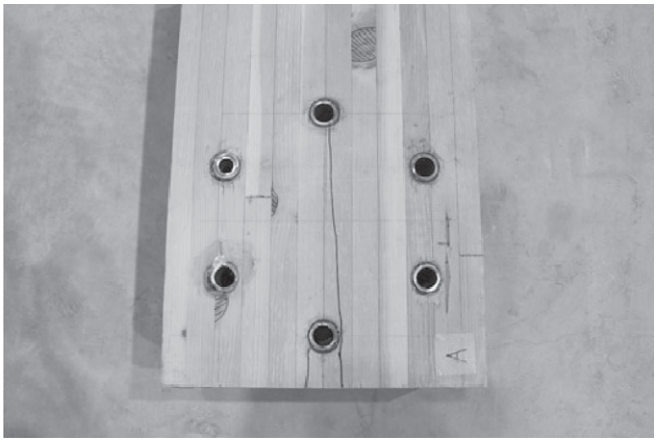

(a)

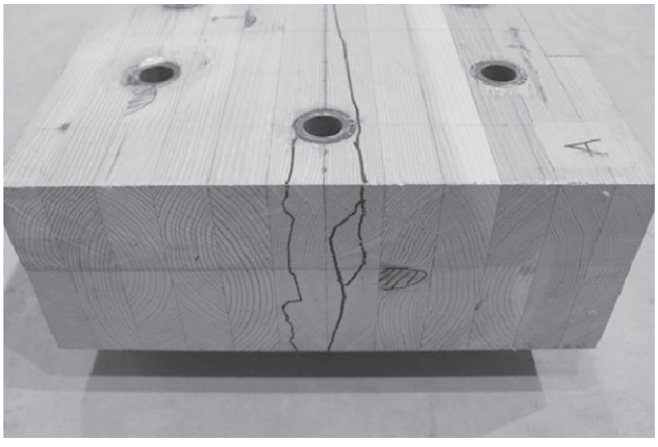

(b)

Fig. 10. Specimen A2 after the test: **a** side view, **b** side and bottom view. The cracks are minute and their positions are indicated with a black marker pen

Table 1. Variation of equivalent viscous damping ratio

ψ (mm)		3.33			6.67			13.33			20.00		
Cycle		1	2	3	1	2	3	1	2	3	1	2	3
ς_{eq} (%)	A1	48.8	34.4	31.6	36.8	43.7	43.5	43.0	43.1	41.3	32.3	32.9	33.9
	A2	45.0	49.4	44.9	39.8	43.3	41.8	38.1	38.2	41.5	35.7	36.3	36.8

ψ, loading amplitude; ς_{eq}, equivalent viscous damping ratio; A1, four-bolt specimen; A2 six-bolt specimen

where n is the number of high-strength bolts, μ (= 0.30) is the average friction coefficient between the aluminum splice plates and the end surfaces of the steel tubes as obtained from the material tests, T is the average value of the bolt tension measured before the quasistatic cyclic loading test, and R is the distance between the center of rotation and the locations of the steel tubes as shown in Fig. 5.

Figures 9 and 10 show specimens A1 and A2 after the test. It should be noted that the cracks in specimen A2 were minute and a black marker pen was used to indicate their locations in Fig. 10. On the other hand, the cracks in specimen A1 were clearly visible and a marker was not used to indicate their locations in Fig. 9. Figure 11 shows the splice plates after the tests, from which evidence of slip can be clearly seen.

Table 1 summarizes the variation in the equivalent viscous damping ratio. The equivalent viscous damping ratio is obtained as:

$$\varsigma_{eq} = \frac{1}{4\pi}\frac{E_h}{E_e}, \tag{4}$$

where E_h is the energy dissipated in one cycle of hysteresis loop and E_e is the strain energy at the maximum rotation angle in the hysteresis loop. Note that E_e is defined using the secant modulus.

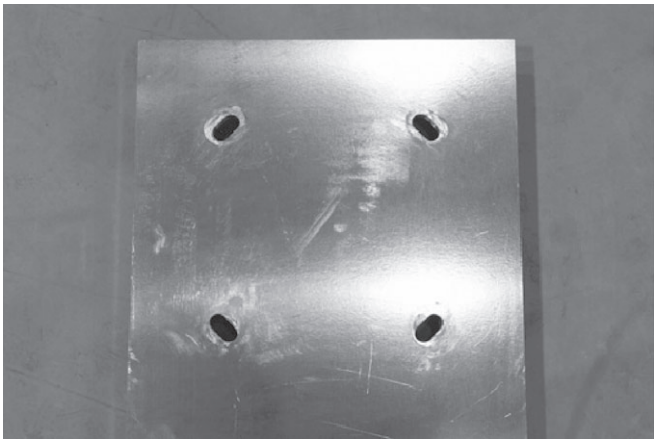

(a)

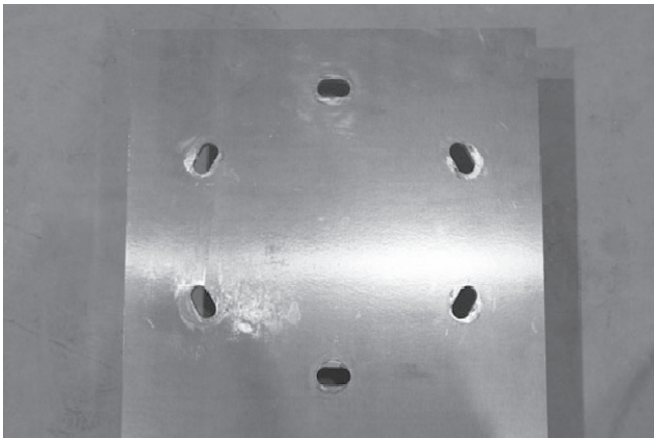

(b)

Fig. 11. Splice plates after the tests showing evidence of slip: **a** specimen A1, **b** specimen A2

From the tests, the following observations were made:

1. Pinching was successfully avoided and nearly rigid–plastic hysteresis loops with a high equivalent viscous damping ratio were obtained in both specimens A1 and A2.
2. The strength capacity ratio, defined as the ratio of the maximum flexural stress corresponding to M_c to the flexural strength of the glulam, were 28.3% and 30.1%, respectively, for specimens A1 and A2. For reference, the ratio of the shear stress to the maximum flexural stress was 16.3% for each specimen.
3. Although partial fracture took place in the glulam as shown in Figs. 9 and 10, no significant drop of restoring moment was observed in the hysteresis loops. This means that the failure mode of the present connection was ductile.
4. The measured value of the amplitude of the rotation angle was significantly smaller than the intended value of the amplitude of rotation angle ψ/h. Possible reasons for the difference are (1) variation of the center of rotation due to the clearance between the high-strength bolts and the curved slots and (2) deformation of the glulam. To resolve this problem, it would probably be effective to provide a pin connection at the center of rotation.[3,5]
5. Unexpected hardening was observed when sliding took place even though the relative rotation angle was smaller than the allowable angle; the moment capacities obtained by the tests were slightly lower than the estimates. Possible reasons for the unexpected hardening and the lower moment capacities are (1) interaction between the shear force and moment, and (2) friction between the side of the high-strength bolts and that of the slots in the splice plates. Providing a pin connection at the center of rotation may also help to resolve these problems.

Conclusions

This note examined the feasibility of an improved slotted bolted connection for timber moment frames. The hysteresis loops obtained from quasistatic cyclic loading tests of the two connection specimens were nearly rigid–plastic with an equivalent viscous damping ratio of more than 30% in the ranges of rotation angle close to or greater than 1/50 radian. Although unexpected hardening was observed during the sliding phase, the experimental results demonstrate the feasibility and potential of the present connection.

The main strengths of the present improved SBC for timber moment frames can be summarized as follows: (1) Compression due to bolt tension is fully supported by steel tubes, which prevents reduction of the energy dissipating capacity due to shrinkage of glulam even in long-term use. (2) The initial stiffness is very high when a timber frame is under normal conditions or subjected to small to moderate earthquakes. On the other hand, stable and large energy dissipation by sliding between steel tubes and aluminum splice plates can be expected when a timber frame is subjected to strong earthquakes.

The issues that need to be addressed in the future include, but are not limited to, the examination of the effect of providing a pin connection at the center of rotation, further improvement of the build-up process, and more comprehensive study of the design conditions for preparing a design guideline of the proposed SBC.

Acknowledgments This research was supported by an Emachu research grant (2009–2010) provided by the Japan Wood Research Society. Mr. Nobutoshi Yoshida, a technical engineer at Kyoto University, helped to conduct the experiments. We gratefully acknowledge this support. Also the authors appreciate the comments from the reviewers, which led to significant improvements of the draft of this article.

References

1. Rodd PD (1988) Timber joints made with new and improved circular dowel connectors. In: Proceedings of the International Timber Engineering Conference, Seattle, vol 1, pp 26–37
2. Guan ZW, Rodd PD (2001) Hollow steel dowels – a new application in semi-rigid timber connections. Eng Struct 23:110–119
3. Leijten AJM, Ruxton S, Prion H, Lam F (2006) Reversed-cyclic behavior of a novel heavy timber tube connection. J Struct Eng 132:1314–1319

4. Thelandersson S, Larsen HJ (2009) Timber engineering. Wiley, Chichester
5. Duff SF, Black RG, Mahin A, Blondet M (1998) Friction damped energy dissipation timber connections. In: Proceedings of the 5th World Conference on Timber Engineering, Montreux, vol 1, pp 361–368
6. Leichti RJ, Tjahyadi A, Bienhaus A, Gupta R, Miller T, Duff, S (2002) Design and behavior of friction dampers for two-dimensional braced and moment-resisting timber frames. In: Proceedings of the 7th World Conference of Timber Engineering, Shah Alam, vol 3, pp 267–274
7. Awaludin A, Hirai T, Hayashikawa T, Sasaki Y, Oikawa A (2008) One-year stress relaxation of timber joints assembled with pretensioned bolts. J Wood Sci 54:456–463
8. Tokuda H, Shigematsu, Y, Kondo K (1990) Timber space structures of "the Japanese government plaza" in the international garden and greenery exposition Osaka, Japan, 1990 (in Japanese). GBRC 59:3–8
9. Suzuki T, Sakata H, Takeuchi T, Matsuoka Y, Nagayama K, Matsuda K (2005) Study on mechanical behavior of glulam timber–steel composite member (in Japanese) In: Summary of Technical Papers of Annual Meeting of AIJ, Osaka, C-1:277–278
10. Japanese Industrial Standard Committee (2006) JIS H4000 (in Japanese). http:// www.jisc.go.jp/app/pager?id=59411, Accessed August 21, 2010
11. Yoshioka T, Ohkubo M (2003) Bending-shear tests of a wide-flange steel beam using the bolted frictional-slippage damper on the bottom flange at the beam end (in Japanese), AIJ J Struct Constr Eng 68(573):177–184
12. Japanese Industrial Standard Committee (2010) JIS G3101 (in Japanese). http:// www.jisc.go.jp/app/pager?id=60578, Accessed August 21, 2010
13. Japanese Industrial Standard Committee (2007) JIS B1186 (in Japanese). http:// www.jisc.go.jp/app/ pager?id=60898, Accessed August 21, 2010